KONINKLIJK NEDERLANDS
METEOROLOGISCH INSTITUUT

VERSLAGEN

V-326

G.J. Cats

Wind profile estimates up to 200 m from synoptic observations

De Bilt, 1979

Publikatienummer: K.N.M.I. V-326 (M.O.)

Koninklijk Nederlands Meteorologisch Instituut,
Afd. Meteorologisch Onderzoek (MO),
Postbus 201,
3730 AE De Bilt,
Nederland.

U.D.C.: 551.501.75

Abstract

A scheme is described for estimating the friction velocity u_* and the Obukhov length L from synoptic observations. Use is made of Businger's flux-profile relationships. The estimated values of u_* are in very good agreement with values obtained from fitting Businger's profiles to observations of wind speed and temperature profiles up to 20 m. The estimated values of L show less agreement, especially during the night. The estimated u_* and L lead to good wind speed estimates up to a height of 200 m in near-neutral conditions. In very unstable conditions the correlation coefficient between estimated and observed wind speeds is small, but, because of the low average wind speed, the root-mean-square error of estimate is also small (<1.7 m/s at 200 m). In very stable conditions the estimation scheme leads to completely erroneous results (at 200 m, e.g. the r.m.s. error of estimate is 4 m/s), because the Businger relations are applied far beyond their application range.

-o-o-o-

1. Introduction

For initialization and evaluation of boundary layer models a boundary layer wind analysis is required. An analysis scheme can make use of wind observations, and if needed, other meteorological observations. In general, very few wind observations are available above the height of 10 m. In order to be able to detect small-scale phenomena above this height, the boundary layer wind analysis scheme will have to take the relatively dense 10 m wind observations into account. These observations, however, should be corrected according to a log-profile, with, if possible, a stability correction.

This report documents an investigation into the possibilities to estimate wind profiles, using only surface observations. First, the net radiation is estimated from the solar height ψ, and cloudiness N. From the net radiation the sensible heat flux H_0 is estimated. The scheme used to estimate H_0 from ψ and N is essentially the same as used by Burridge and Gadd (1975). The experimental relation, found by Businger et al. (1971), then is used to estimate the wind speed at the height z from the 10 m wind speed u_{10}, the sensible heat flux H_0 and the surface roughness z_0. This relation reads:

$$u_z = \frac{u_*}{k} \left(\ln \frac{z}{z_0} - \Psi\left(\frac{z}{L}\right)\right) \qquad (1)$$

where u_* is the friction velocity, L is the Obukhov length:

$$L = - \frac{T}{g} \frac{u_*^3}{k} \frac{\rho c_p}{H_0} , \qquad (2)$$

$$\left.\begin{array}{l} \Psi(\zeta) = 2 \ln ((1+\xi)/2) + \ln((1+\xi^2)/2) - \\ \qquad 2 \arctan \xi + \pi/2 \qquad\qquad (\zeta < 0) \\ \qquad (\text{with } \xi = (1-15 \zeta)^{\frac{1}{4}}) \\ (\text{approximated by } \Psi(\zeta) = 1.08 (-\zeta)^{\frac{1}{2}} \text{ (Van Ulden, 1977)).} \\ \Psi(\zeta) = -4.7\zeta \qquad (\zeta > 0) \end{array}\right\} \quad (3)$$

Further, H_0 is the sensible heat flux, k is de Von Kármán constant (in Businger's relation (3) the value

$$k = 0.35 \tag{4}$$

has to be used), T is a representative surface layer temperature, g is the gravity acceleration ($g = 9.81\ m/s^2$), ρ is the air density and c_p the specific heat capacity of air ($\rho c_p = 1240\ JK^{-1}m^{-3}$). The friction velocity u_* can be determined iteratively from (1) and (2) for $z = 10$ m, if values of z_0, H_0 and u_{10} are given. The solution of and some problems arising in this iteration process are discussed in section 3.

The wind profile estimation scheme was evaluated by comparing estimated and observed wind speed at heights between 20 and 200 m. Below 20 m, the scheme was verified in an alternative way. Estimated values of u_* and L were compared with values that were obtained from a least-square-best fit of the Businger (1971) wind and temperature profiles to observations up to 20 m (Nieuwstadt, 1978). Throughout this paper, the latter values of u_* and L are denoted by "calculated" and the values from the estimation scheme by "estimated". Because both estimated and calculated u_* values depend heavily on the common use of the 10 m wind speed u_{10} and the surface rougnness z_0, a high correlation between estimated and calculated values is expected. The Obukhov length L, however, is found in two independent ways: in the estimation scheme from estimated heat fluxes and in Nieuwstadt's calculation from the vertical wind and temperature gradients.

In section 2 of this report the data set used for the evaluation is described. In section 3 some further remarks on the used flux-profile relations are made. Section 4 describes the scheme for estimation of H_0. In section 5 the verification results are given.

2. The data set

During the period 1-3-1977 till 1-3-1978 observations of wind speed at the heights of 200, 160, 120, 80, 40, 20, 10, 5 and 1.5 m and of temperature at the heights of 20, 10, 5, 2 and 0.6 m were performed along the mast at Cabauw (Driedonks et al., 1978). The observations were averaged over half hours. For each wind direction sector of 30° the surface roughness z_0 was objectively determined from a gust factor analysis (Wieringa, 1976). In the wind directions between 20° and 140°, however, this analysis was not reliable, because a row of trees had been cut down between the period over which gust factors were determined and the abovementioned year. These directions were therefore rejected.

Further observations at Cabauw include the net radiation R_N. Cloudiness and relative humidity were taken from four synoptic stations surrounding Cabauw. (Average distance to Cabauw 35 km). The observations at these stations were averaged to form an estimate for the cloudiness at Cabauw.

All observations that were required in this research were simultaneously available during more than 10000 half hours.

3. The flux-profile relationships

The Businger flux-profile relationship (1-4) leads to a relation between the stability parameter

$$s = \frac{k u_{10}}{u_* \ln(z/z_0)} \qquad (5)$$

and the from observations available quantity

$$x = \Psi\left(-k \frac{zg}{T} \frac{H_0}{\rho c_p} \left(\frac{\ln(z/z_0)}{ku}\right)^3\right) / \ln(z/z_0) \qquad (6)$$

(with Ψ according to (3)). This relation is plotted in figure 1.

During unstable conditions is $H_0 > 0$, $x < 0$ and, therefore, $s < 1$. During stable conditions two solutions of s exist, if $x < 4/27$. One corresponds to slightly stable stratification

$(1 < s \leqslant 1.5)$ and one to very stable conditions $(s \geqslant 1.5)$. This double solution may be understood physically by realizing that H_0 is dependent on turbulence intensity. For, if K-theory is assumed:

$$\frac{H_0}{\rho c_p} = - K \frac{\partial \theta}{\partial z} \tag{7}$$

A small $|H_0|$ may be caused by a small $\frac{\partial \theta}{\partial z}$ (near-neutral stratification). However, K is proportional to the turbulence-intensity scale u_*. A small $|H_0|$ may therefore also be caused by a small u_*, which is associated with very stable stratification.

From figure 1 it is also seen that Businger's relation leads only to estimates for u_* if $x \leqslant 4/27$. In actual situations observations may well lead to a calculated x exceeding 4/27. In the data set used this occurred in 717 half hours (about 7%). (If H_0 is estimated conforming to section 4). The flux-profile relationship proposed by Carson and Richards (1978) has a larger applicability range: only in 457 hours no fluxes could be calculated using this relation.

4. Sensible heat-flux estimation scheme

The sensible heat flux H_0 was estimated according to the following scheme:

An "effective cloudiness" was formed by averaging total and low cloud cover:

$$N_{av} = (N + N_L)/2 \tag{8}$$

to give a lower weight to high than to low clouds.

The net radiation was written as

$$R_N = (R_0^{\downarrow} - R_0^{\uparrow})(1 - 0.9\, N_{av}) \tag{9}$$

with the net shortwave radiation

$$R_0^{\downarrow} = (1 - \alpha)\, S^{\downarrow}\, T_a(\psi) \sin \psi \tag{10}$$

and the net longwave radiation

$$R_0^\uparrow = S^\uparrow \; (T/T_a)^4 \qquad (11)$$

In here ψ is the solar height (replaced by 0 if the sun is below the horizon), T_a is the atmospheric transmissivity, taken as

$$T_a(\psi) = 0.6 + 0.2 \sin \psi \qquad (12)$$

α is the surface albedo, taken to be

$$\alpha = 15\% \qquad (13)$$

$S^\downarrow$ is the solar constant

$$S^\downarrow = 1350 \text{ W/m}^2 \qquad (14)$$

T is the air temperature, and T_0 was chosen

$$T_0 = 285 \text{ K} \qquad (15)$$

The constant $S^\uparrow$ was taken

$$S^\uparrow = 91 \text{ W/m}^2 \qquad (16)$$

The constants in (9) through (16) are taken from Burridge and Gadd (1975). Some modifications, however, were required, for example, because only total and low cloud cover are available, whereas Burridge and Gadd require high, medium and low cloud cover to be known separately. The constant 0.9 in (9) and the form of (11) with (15) were chosen as a first guess.
From the net radiation R_N, the sensible heat flux was estimated as

$$H_0 = 0.4 \; R_N \qquad (17)$$

which, for its simplicity, was preferred to the Burridge and Gadd scheme. The constant 0.4 was chosen as an average of observations at Cabauw.

To test the sensitivity of the estimation scheme to (17), some other equations were also used.

With the above-described scheme, H_0 is expressed in terms of the synoptic observations of temperature, cloudiness and time of day and year.

5. Results

a. Comparison of calculated and estimated u_* and L

For each half hour for which $x < 4/27$ (see Eq. 6) the friction velocity u_* and the Obukhov length L were estimated with the formulae given in section 4. Further, values of u_* and L were calculated by least square fitting of the Businger profile to the observations up to the height cf 20 m (Nieuwstadt, 1978). A comparison of estimated and calculated values has led to the following linear regression equations:

$$u_*(\mathrm{est}) = 0.945\ u_*(\mathrm{calc}) + 0.035\ \mathrm{m/s} \qquad (18)$$

(correlation coefficient between $u_*(\mathrm{est})$ and $u_*(\mathrm{calc})$ 0.989)

$$1/L(\mathrm{est}) = 0.96\ 1/L(\mathrm{calc}) - 6.5\ 10^{-3}\mathrm{m}^{-1} \qquad (19)$$

(correlation coefficient 0.68).

Indeed a high correlation coefficient is found between estimated and calculated u_* (see introduction). The slopes of the regression lines are almost equal to 1 (as they should).

In cases with ambiguity in the choice of u_* ($H_0 < 0$, see fig. 1) the higher value of u_* was chosen, because 1) only very occasionally the lower value of u_* was nearer to the calculated value than the higher, and 2) no independent criterion was found to choose between the two choices.

Some tests were performed to investigate the sensitivity of the estimation scheme to the parameters introduced in Eqs. 8 to 17. The scheme turned out to be quite insensitive. A slight improvement was found by using a variable partitioning of the net radiation over sensible and latent heat flux, amounting to the replacement of (17) by

$H_0 = 0.23\ R_N$ during precipitation, and

$H_0 = 0.50\ R_N$ else.

The scheme appeared not to improve the results when (17) was replaced by a procedure to estimate soil heat flux and latent heat flux (the former according to Burridge and Gadd (1975), taken as

$G = 0.1\ R_N$ if $R_N > 0$, and

$G = 0.5\ R_N$ else,

and the latter calculated with Penman's (1948) method under the assumption of the surface to be wet). In one run, the procedure to estimate R_N was replaced by observations of R_N. This did not lead to any improvement, from which it is concluded that the net radiation scheme (Eqs. (8) to (16)) is sufficiently accurate for our purposes. The main errors are introduced in (17), and, of course, in the assumption of the validity of Businger's profile in real-life (i.e. non-stationary, non-homogeneous) conditions. (Both estimated and calculated u_* and L then will be erroneous, but in general the errors will not cancel, due to the different ways of obtaining estimated and calculated values).

In order to make the scheme for estimation of u_* and L applicable for all values of x, x was replaced by 4/27 in cases when it exceeded this value. This procedure reduced the correlation between estimated and calculated 1/L to 60%. The scheme behaved considerably better during day-time than during night-time ($H_0 < 0$). This may be caused by the fact that the linear relation between H_0 and R_N (Eq. (17)) is too much a simplification during night-time (e.g. due to soil heat flux) and by the - rare - wrong choice out of the two possible u_* values.

In figures 2, 3 and 4 scatter diagrams are given of estimated versus calculated u_* and 1/L for midday (1200 GMT) and midnight. During these hours the scheme is significantly better than during the whole data set. This indicates that especially during the day-night and night-day transition hours the scheme may lead to erroneous estimates for u_* and L. However, during the transition hours the calculated L-values may equally well be in error, for example due to wrong temperature gradient estimates caused by dew on the sensors.

b. Comparison of wind speed profiles

Once u_* and L are known, Eq. (1) leads to an estimate for wind speed at an arbitrary height within the surface layer. In the following, the height of this surface layer is estimated as the height up to which the estimated wind speed agrees with observations. Conforming the preceding sections u_* and L were calculated from synoptic observations and an objective estimate of the surface roughness z_0. The estimated wind speed was compared with observations at every observation height above 20 m (inclusive).

The data set described in section 2 was divided into five classes, according to the estimated value of the Obukhov length L. These classes are:

(a) Very unstable : $-10 \text{ m} \leqslant L < 0$
(number of half hours: n = 125)
(b) Unstable : $-1000 \text{ m} \leqslant L < -10 \text{ m}$ (n = 3300)
(c) Near-neutral : $|L| > 1000 \text{ m}$ (n = 3400)
(d) Stable : $50 \text{ m} < L \leqslant 1000 \text{ m}$ (n = 2600)
(e) Very stable : $0 < L \leqslant 50 \text{ m}$ (n = 1800)

The numbers of half hours are approximate, because not at every height the same number of observations was available.

In cases with very low observed wind speed $|L|$ may reach very small values. This often led to completely erroneous wind speed estimates at most heights. Empirically it was found that, in the calculation of L, u_* had to be taken at least 0.10 m/s. Further, in the very unstable and very stable cases L was replaced by -10 m and 50 m respectively.

In figure 5 the root-mean-square difference between estimated and observed wind speeds is indicated. This difference is seen to be about 2 m/s at the height of 200 m, except in stable and very stable conditions. In figure 5 the correlation coefficient between estimated and observed wind speeds is denoted by full lines. This coefficient is high in near-neutral conditions (at 200 m it is 87%), but in both stable and unstable conditions it decreases sharply. Because of the associated low values of $|L|$ the surface layer is only shallow, and the break-down of the Businger relations has to be expected. In these cases knowledge of the boundary layer height will be essential. Yet, the root-mean-square error-of-estimate is small, because in the very stable and unstable conditions the average wind speed is low.

From figure 5 it is inferred to what height Businger's relation, with the described H_0 estimation scheme, is applicable if one requires a certain accuracy. If, for example, it is required that the correlation coefficient exceed 90%, the estimates are applicable up to the height of 0.5 $|L|$.

In figure 6 scatter diagrams of estimated versus observed 200 m wind speeds are given for the five stability classes. In the very unstable case some high 200 m wind speeds occur. In these cases the surface layer did not extend up to 200 m. In the two cases plotted an inversion at a height of about 170 m was found by sonic detection. At greater heights, as compared to $|L|$, a wind speed estimation scheme can only hoped to be reliable if it uses information on boundary layer height.

In the above, attention has been given only to wind speed estimates. It was found empirically that the estimation scheme performed as well when applied to the wind component parallel to the 10 m wind. The component perpendicular to the 10 m wind was in general small. No reliable estimation scheme for this component was found. It is suggested, therefore, to estimate the wind speed with the above-described scheme, and the wind direction by taking it equal to the 10 m wind direction, apart from a small climatological veering. This scheme is applicable up to a height which is inferred from figure 5.

6. Conclusions

With the flux-profile relationship proposed by Businger et al. (1971) and the sensible heat flux estimation scheme of Burridge and Gadd (1975) the friction velocity u_* and the Obukhov length L can be estimated. The estimated u_* agrees well with values obtained from a least-square best fit of Businger's relations to observed wind and temperature profiles (Nieuwstadt, 1978), but L shows less agreement.

The estimated values of u_* and L lead to good wind speed profile estimates up to a height which is a certain fraction - depending on the accuracy required - of the estimated absolute value of L. This fraction, for example, is more than ½ if the required correlation coefficient is 90%.

Therefore it is concluded that the described scheme is very useful in wind analysis problems. To obtain an estimate of wind speed and direction at heights above, say, 0.5 $|L|$, however, the scheme will have to be replaced by a more sophisticated one, which e.g. takes into account the boundary layer height.

Acknowledgments

I am indebted to A.P. van Ulden, H.A.R. de Bruin and W. Kohsiek for many useful advices, and to S. Kruizinga for providing his regression analysis algorithms.

References

Burridge, D.M. and A.L. Gadd, 1975: The Meteorological Office Operational 10-level Numerical Weather Prediction Model (December 1975), Meteorological Office Scientific Paper No. 34.

Businger, J.A., J.C. Wyngaard, Y. Izumi and E.F. Bradley, 1971: Flux Profile Relationships in the Atmospheric Surface Layer, J. Atmosph. Sci. 28, 181-189.

Carson, D.J. and P.J.R. Richards, 1978: Modelling Surface Turbulent Fluxes in Stable Conditions, Boundary Layer Meteorol. 14, 67-81.

Cats, G.J., 1978: Surface wind analysis over land in the Netherlands, based on an optimum interpolation method, K.N.M.I. Publication W.R. 78-17.

Driedonks, A.G.M., H. van Dop and W.H. Kohsiek, 1978: Meteorological Observations on the 213 m mast at Cabauw in the Netherlands. Proceedings of the 4th symposium on meteorological observations and instrumentation, Denver.

Hicks, B.B., 1976: Wind Profile Relationships from the "Wangara" Experiment, Quart. J. Roy. Meteorol. Soc. 102, 535-551.

Nieuwstadt, F.T.M., 1978: The Computation of the Friction Velocity u_* and the Temperature scale T_* from Temperature and Wind Velocity Profiles by Least-Square Methods, Boundary Layer Meteorol. 14, 235-246.

Penman, H.L., 1948: Natural Evaporation from Open Water, Bare Soil and Grass, Proc. Roy. Soc. A. 193, 120-146.

Van Ulden, A.P., 1977: Private communication.

Wieringa, J., 1976: An Objective Exposure Correction Method for Average Wind Speed Measured at a Sheltered Location, Quart. J. Roy. Meteorol. Soc. 102, 241-253.

-o-o-o-

Figure captions

Fig. 1. The stability parameter $s = ku/(u_* \ln(z/z_0))$ as a function of the parameter x, which depends on sensible heat flux H_0, surface roughness z_0 and wind speed u at height z. The function Ψ is given in Eq. 6. For $x < 0$ ($H_0 > 0$) a logarithmic x-scale is used, for $x > 0$ a linear scale.

Fig. 2. Scatter diagram of estimated versus calculated friction velocity u_* at 1200 GMT. The line shows the linear regression $u_*(\mathrm{est}) = a\, u_*(\mathrm{calc}) + b$ with $a = 0.94$, $b = 0.042$ m/s. The number of observations is $n = 249$ and the correlation coefficient $r = 0.989$.

Fig. 3. As fig. 2, however at 2400 GMT.
$a = 0.95$, $b = 0.022$ m/s, $n = 191$, $r = 0.990$

Fig. 4 Scatter diagram of estimated 1/L versus calculated 1/L at 1200 GMT (estimated $1/L < 0$) and at 2400 GMT (estimated $1/L > 0$). The regression results are:
1200 GMT : $a = 0.93$, $b = -5.10^{-3} m^{-1}$, $n = 249$, $r = 0.83$
2400 GMT : $a = 1.46$, $b = -3.10^{-3} m^{-1}$, $n = 191$, $r = 0.70$
1200 and 2400 GMT simultaneously:
$a = 1.15$, $b = -1.10^{-3} m^{-1}$, $n = 440$, $r = 0.78$

Fig. 5 Root-mean-square difference (numbers, m/s) and correlation coefficient (lines, per cents) between estimated and observed wind speeds as dependent on height, for the total data set and per class of estimated stablity.

Fig. 6 Scatter diagrams of estimated versus observed 200 m wind speeds for the five stability classes, according to the estimated Obukhov length L. Only the observations during the month of March 1977 are plotted. The indicated lines of best fit, however, are for the whole set (1-3-77 till 1-3-78).
——: Best fit; --- : $y = x$

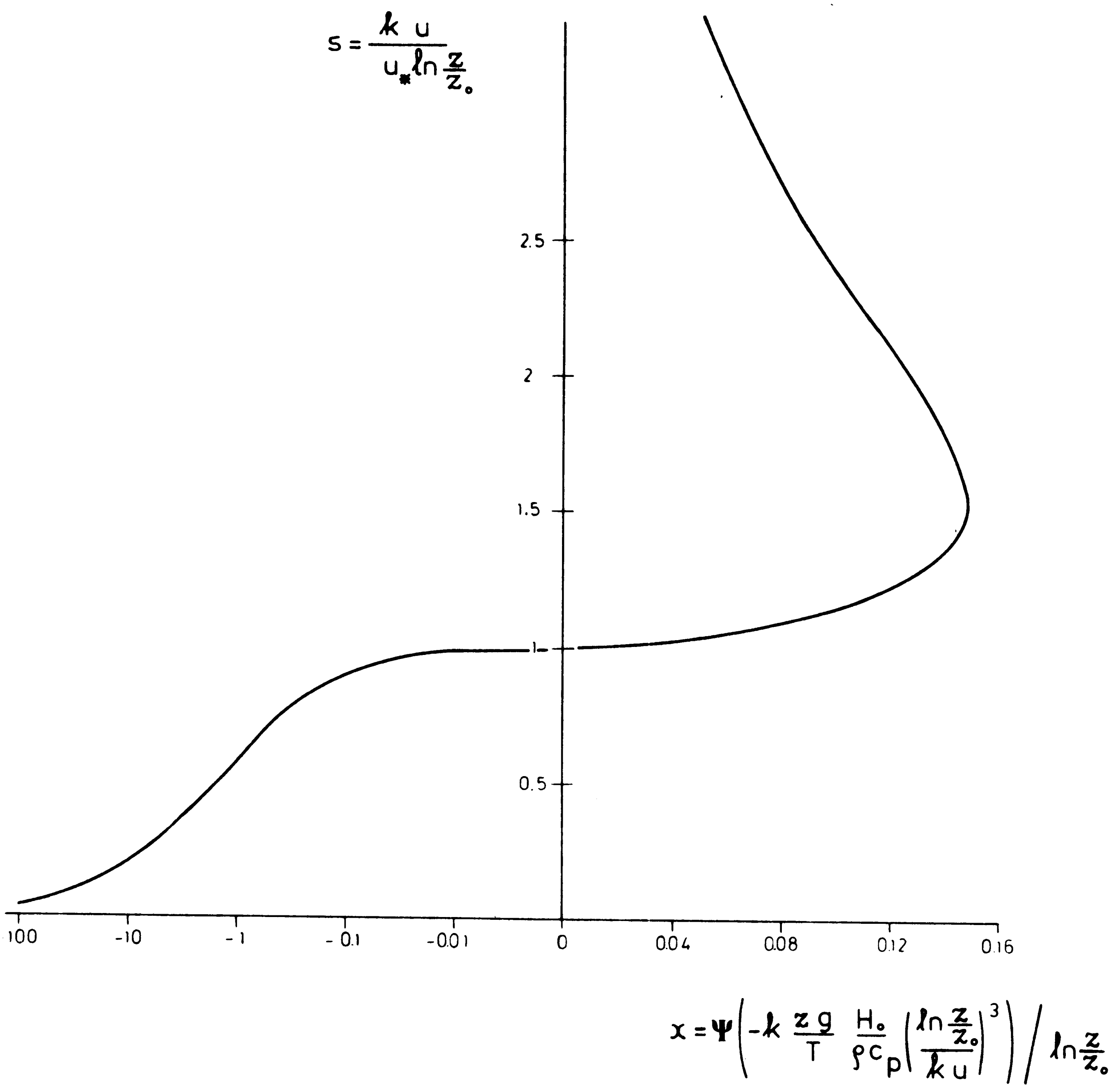
$s = \frac{k\,u}{u_* \ln \frac{z}{z_0}}$
2.5
2
1.5
1
0.5
-100
-10
-1
-0.1
-0.01
0
0.04
0.08
0.12
0.16
$x = \Psi\left(-k\,\frac{z\,g}{T}\,\frac{H_0}{\rho c_p}\left(\frac{\ln\frac{z}{z_0}}{k\,u}\right)^3\right) \Big/ \ln\frac{z}{z_0}$

fig. 1

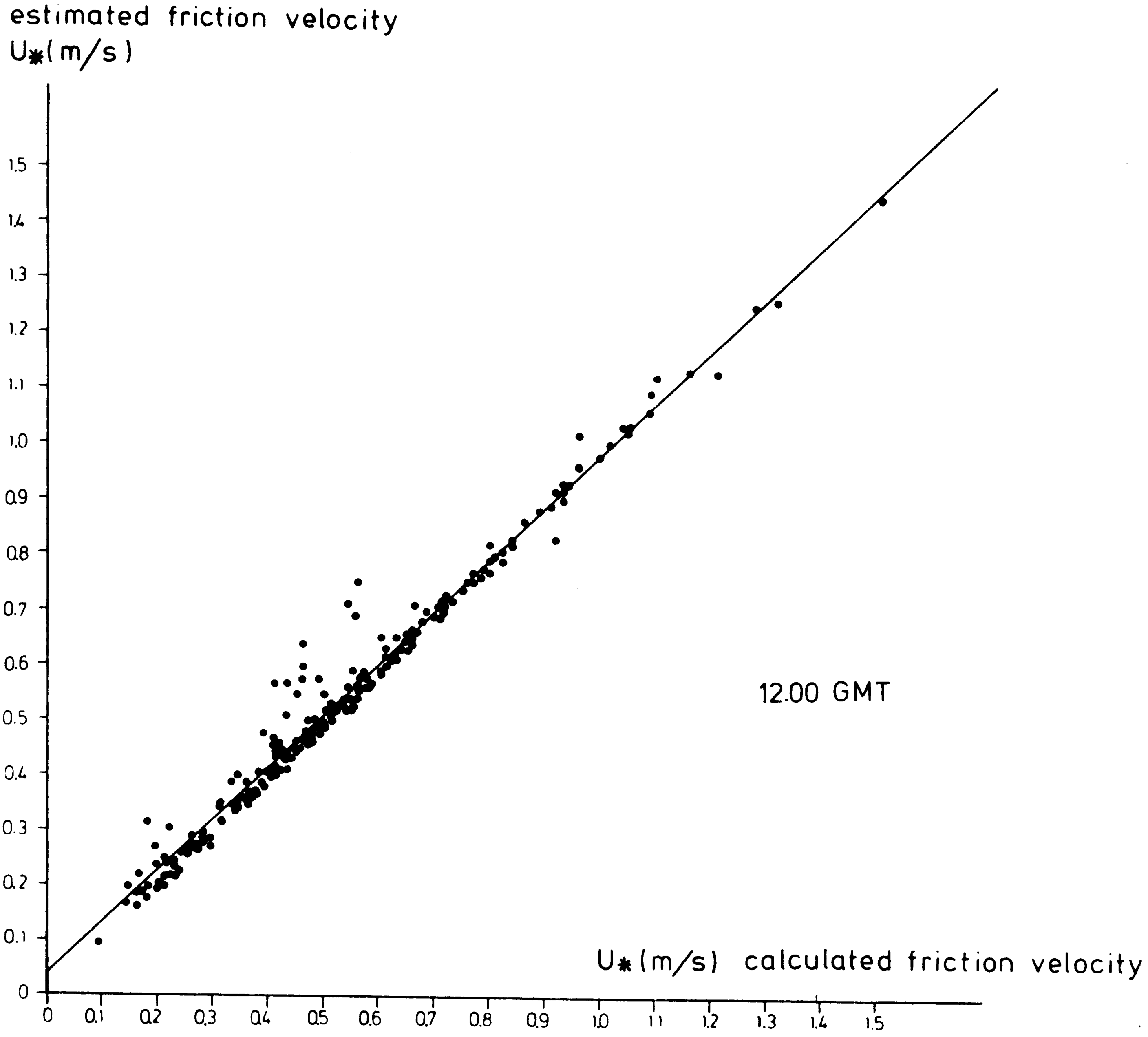
estimated friction velocity
U* (m/s)
1.5
1.4
1.3
1.2
1.1
1.0
0.9
0.8
0.7
0.6
0.5
0.4
0.3
0.2
0.1
0
12.00 GMT
U* (m/s) calculated friction velocity
0
0.1
0.2
0.3
0.4
0.5
0.6
0.7
0.8
0.9
1.0
1.1
1.2
1.3
1.4
1.5

fig. 2

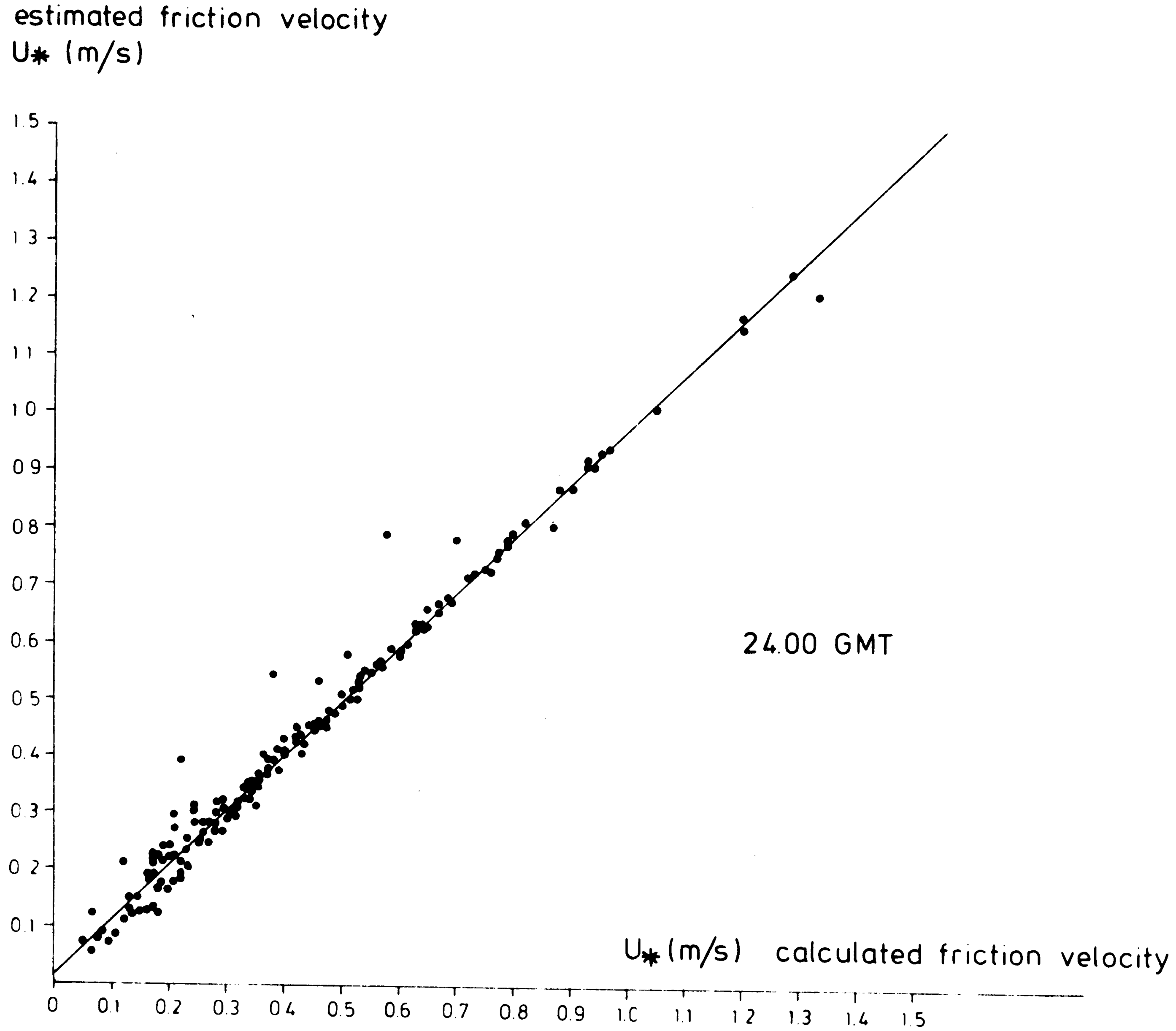
estimated friction velocity
U* (m/s)
1.5
1.4
1.3
1.2
1.1
1.0
0.9
0.8
0.7
0.6
0.5
0.4
0.3
0.2
0.1
24.00 GMT
U* (m/s) calculated friction velocity
0
0.1
0.2
0.3
0.4
0.5
0.6
0.7
0.8
0.9
1.0
1.1
1.2
1.3
1.4
1.5

fig. 3

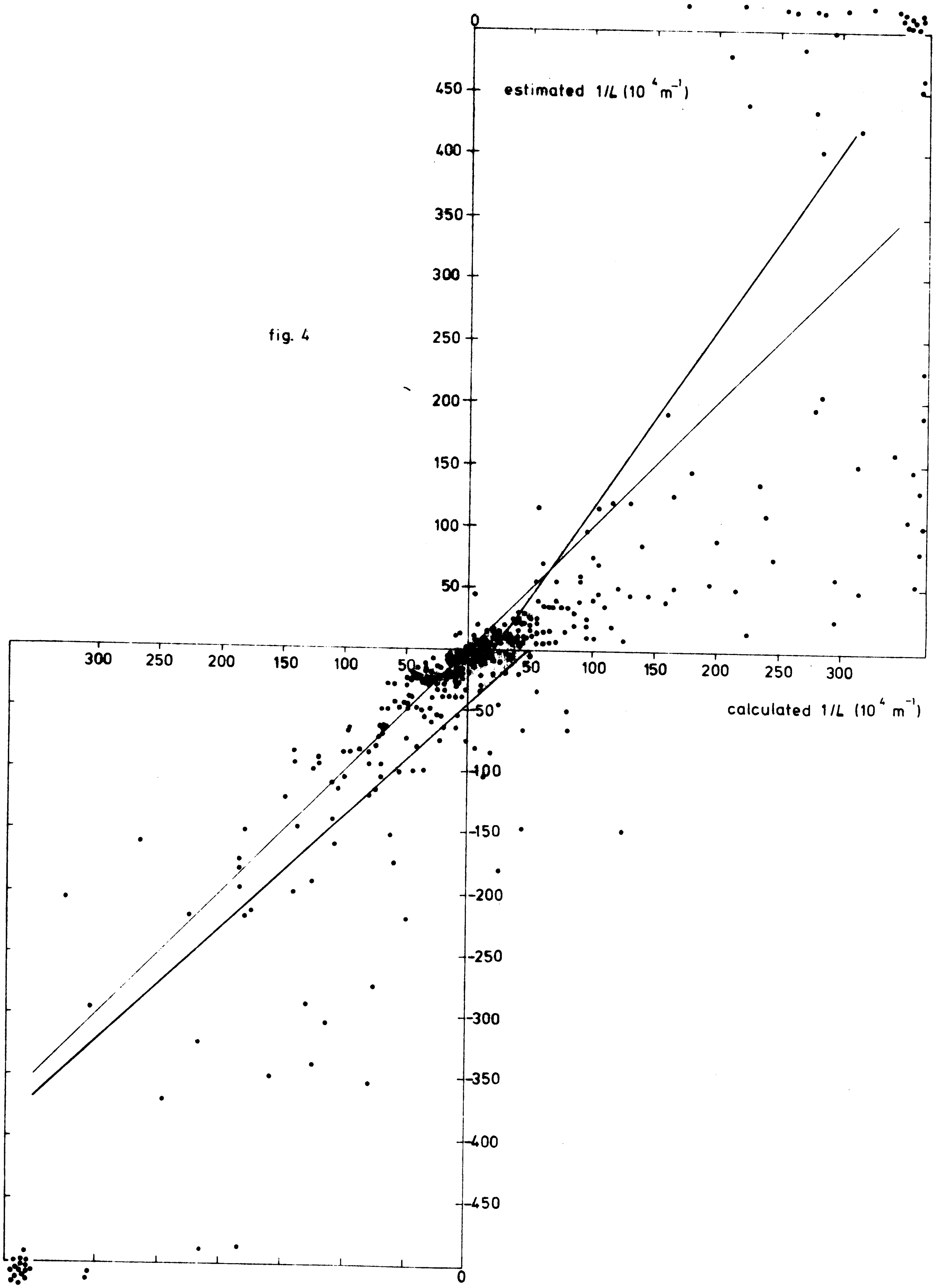
estimated 1/L (10^{4} m^{-1})
calculated 1/L (10^{4} m^{-1})
0
450
400
350
300
250
200
150
100
50
50
100
150
200
250
300
300
250
200
150
100
50
-50
-100
-150
-200
-250
-300
-350
-400
-450
0

fig. 4

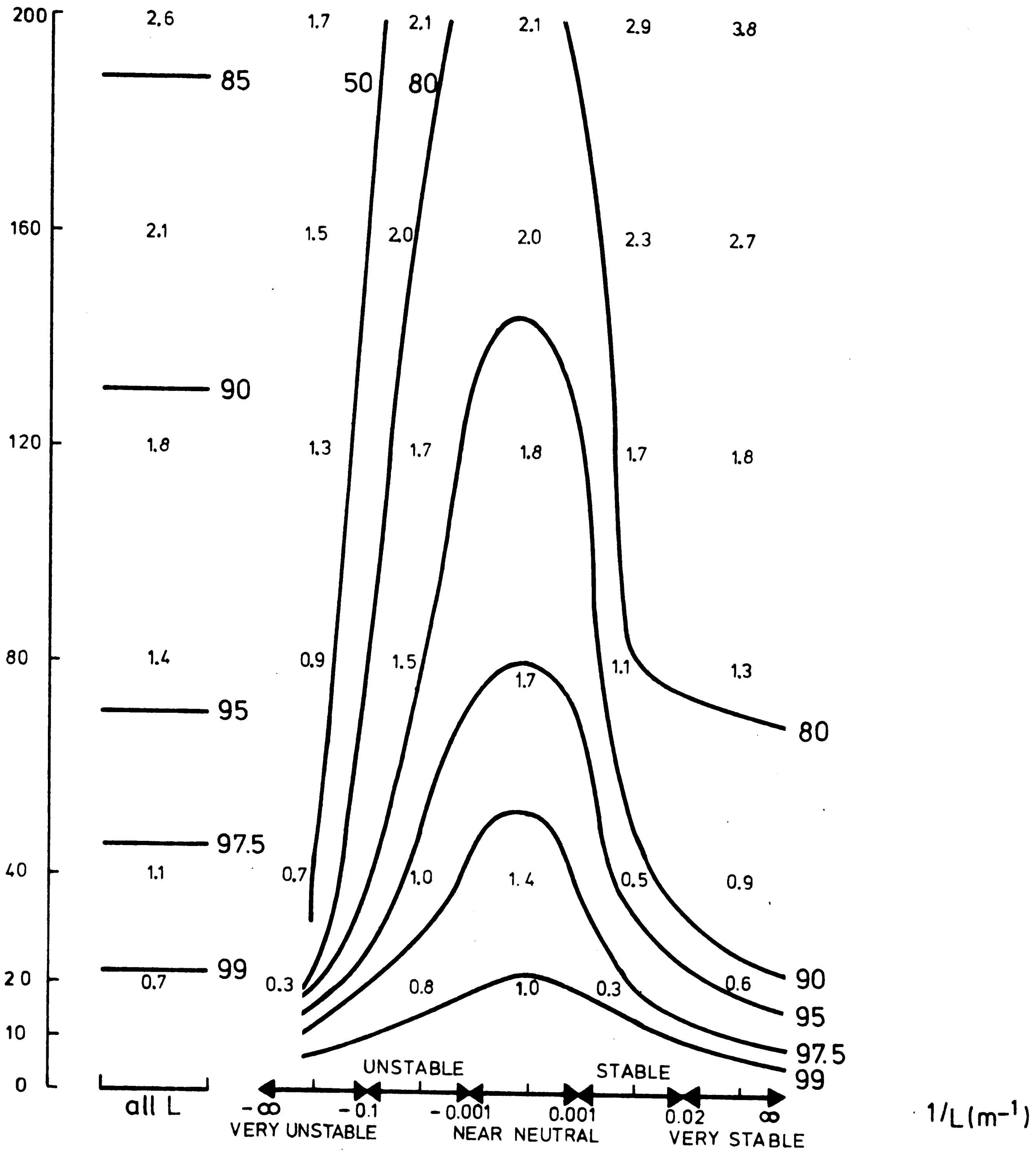

200
160
120
80
40
20
10
0
all L
85
90
95
97.5
99
2.6
2.1
1.8
1.4
1.1
0.7
1.7
1.5
1.3
0.9
0.7
0.3
2.1
2.0
1.7
1.5
1.0
0.8
2.1
2.0
1.8
1.7
1.4
1.0
2.9
2.3
1.7
1.1
0.5
0.3
3.8
2.7
1.8
1.3
0.9
0.6
50
80
80
90
95
97.5
99
UNSTABLE
STABLE
-∞
-0.1
-0.001
0.001
0.02
∞
VERY UNSTABLE
NEAR NEUTRAL
VERY STABLE
1/L(m^{-1})

figs

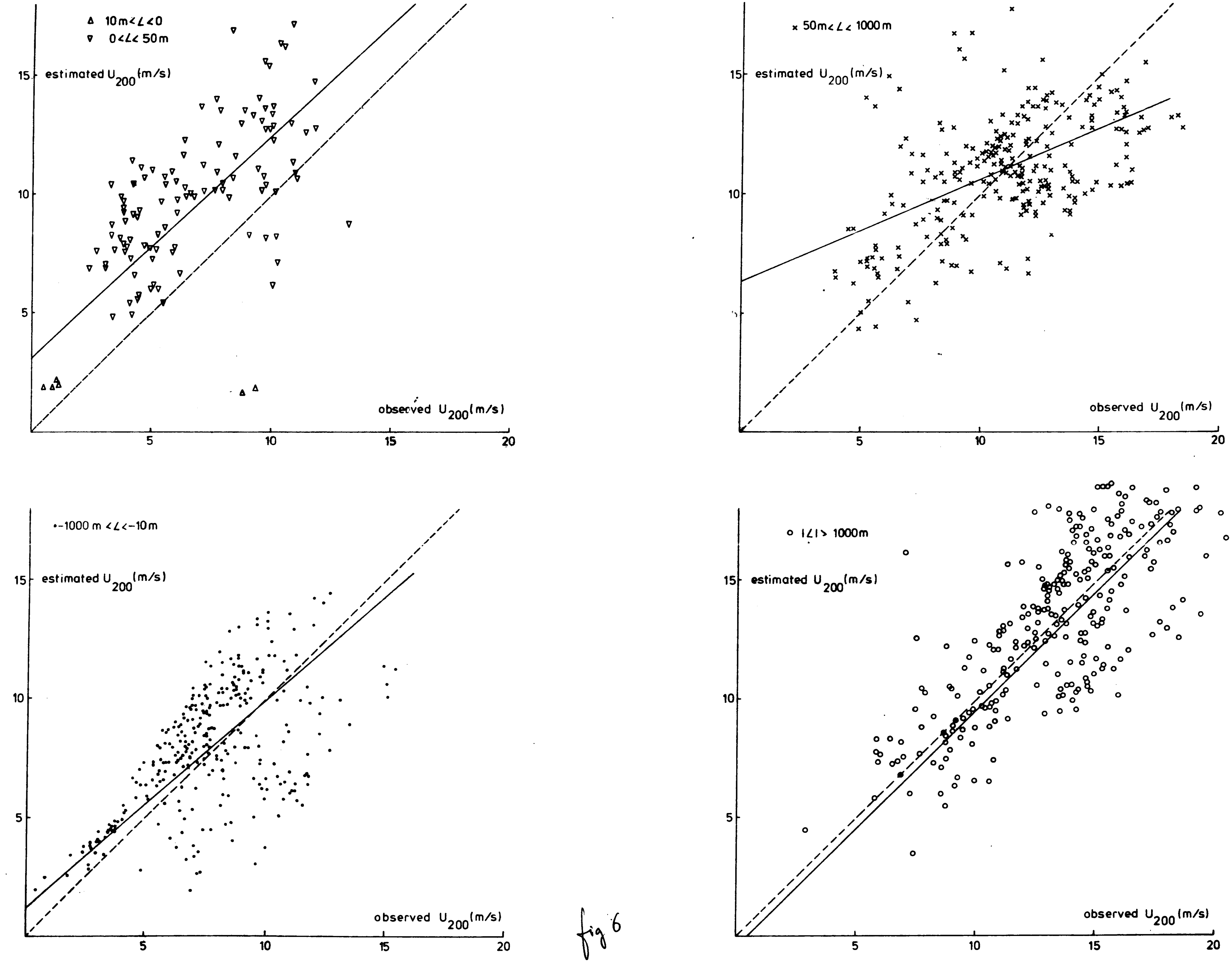

10m< L <0
0< L < 50m
estimated U200 (m/s)
observed U200 (m/s)
5
10
15
20
× 50m< L < 1000m
• -1000 m < L < -10m
○ |L| > 1000m

fig 6